

# Imaging of Retinal Vascular Layers: Adaptive Optics Scanning Laser Ophthalmoscopy Versus Optical Coherence Tomography Angiography

Yoshihiro Kaizu<sup>1</sup>, Shintaro Nakao<sup>1</sup>, Iori Wada<sup>1</sup>, Muneo Yamaguchi<sup>1</sup>, Kohta Fujiwara<sup>1</sup>, Shigeo Yoshida<sup>1</sup>, Toshio Hisatomi<sup>1</sup>, Yasuhiro Ikeda<sup>1</sup>, Takehito Hayami<sup>2</sup>, Tatsuro Ishibashi<sup>1</sup>, and Koh-hei Sonoda<sup>1</sup>

<sup>1</sup> Department of Ophthalmology, Graduate School of Medical Sciences, Kyushu University, Fukuoka, Japan

<sup>2</sup> Department of Intelligent Mechanical Systems, Graduate School of Natural Science and Technology, Okayama University, Okayama, Japan

**Correspondence:** Shintaro Nakao, MD, PhD, Kyushu University 3-1-1 Maidashi, Higashi-Ku, Fukuoka 812-8582, Japan. e-mail: snakao@med.kyushu-u.ac.jp

**Received:** 13 April 2017

**Accepted:** 03 July 2017

**Published:** 1 September 2017

**Keywords:** optical coherence tomography; angiography; vascular plexus; retinal vasculature

**Citation:** Kaizu Y, Nakao S, Wada I, Yamaguchi M, Fujiwara K, Yoshida S, Hisatomi T, Ikeda Y, Hayami T, Ishibashi T, Sonoda K-H. Imaging of retinal vascular layers: adaptive optics scanning laser ophthalmoscopy versus optical coherence tomography angiography. *Trans Vis Sci Tech.* 2017;6(5):2, doi:10.1167/tvst.6.5.2  
Copyright 2017 The Authors

**Purpose:** Retinal vascular networks are observed as a layered structure residing in a nerve fiber layer and an inner nuclear layer of the retina. This study aimed to evaluate reflectance confocal adaptive optics scanning laser ophthalmoscopy (AO-SLO) for imaging of the layered retinal vascular networks.

**Methods:** This study included 16 eyes of 16 healthy cases. On the fovea, 2.8- and 3.0 mm<sup>2</sup>-areas were imaged using a prototype AO-SLO and optical coherence tomography angiography (OCTA), respectively. AO-SLO images focused on the nerve fiber and photoreceptor layers were recorded in the area. Two different vessel images (capillary networks in the superficial layer and in all layers) were generated to examine if the deep capillary network could be distinguished. We compared AO-SLO with OCTA in imaging of the layered retinal vascular networks.

**Results:** Sufficient images of capillary networks for analysis could be generated when the motion contrast was enhanced with AO-SLO movies in seven cases (43.8%). The deep capillary network could be distinguished in the merged image. Vascular depiction performance in AO-SLO was significantly better than in OCTA at both 0.5- and 1.0-mm areas from the fovea ( $P < 0.05$ ).

**Conclusions:** Retinal vascular imaging using AO-SLO might be a useful adjunct to OCTA as a supportive method to evaluate the retina in healthy patients and patients with disease.

**Translational Relevance:** In cases requiring accurate and detailed retinal vasculature observation, AO-SLO might be useful for evaluating retinal vascular lesions as a supportive imaging method of OCTA.

## Introduction

Retinal blood vessels are formed in a hierarchical structure.<sup>1</sup> During vascular development, the first vessels originate at the optic nerve head and spread over the inner surface of the retina, forming a superficial capillary network. After the vascular network has spread to the periphery, vessels start to sprout downward into the deeper layer and the second capillary network in the inner plexiform layer is formed as a deep capillary network.<sup>1</sup>

Fluorescein angiography (FA) has been an established method for observing fine details of the retinal vasculature and early pathologic changes.<sup>2</sup> However, FA requires injection of a fluorescent dye and could cause adverse effects including anaphylaxis.<sup>3</sup> Therefore, frequent follow-up examination should be avoided in patients. Furthermore, FA fails to detect a significant fraction of capillaries, especially those with small diameters, because of its poor depth sectioning capability and sensitivity to the angiogram quality.<sup>4,5</sup>

Recently, various reports have shown that optical coherence tomography angiography (OCTA) could

be useful to examine the retinal vasculatures and its hierarchical structure.<sup>6,7</sup> Spaide et al.<sup>8</sup> also reported its superiority compared with FA in visualization of the retinal capillary layer. However, the horizontal resolution of OCT is known to be around 20  $\mu\text{m}$ , which could be larger than the diameter of retinal capillaries.<sup>9,10</sup>

Adaptive optics scanning laser ophthalmoscopy (AO-SLO) is a technique that enables observation of the retina at the cellular level in patients.<sup>11</sup> Although optical fundus imaging equipment applying adaptive optics including AO-SLO have been mostly employed to visualize photoreceptors,<sup>12–18</sup> it has also been applied to the visualization of vascular features in both normal retina and retina in vascular disorders.<sup>19–22</sup> Furthermore, because the depth of focus is approximately 60  $\mu\text{m}$ , which is calculated from the incident light wavelength (840 nm) and the numerical aperture (0.12),<sup>23</sup> AO-SLO could be useful in imaging a specific layer of the retinal capillary network. Recently, Mo et al.<sup>24</sup> published a study on the difference between OCTA and AO-SLO FA in imaging foveal microvasculatures. However, the utility of AO-SLO in imaging the hierarchical structure of the retinal capillary network has not been well studied. Furthermore, the difference between OCTA and AO-SLO vascular imaging with motion contrast enhancement has not yet been examined.<sup>20</sup> In this study, we evaluated the ability of reflectance confocal AO-SLO to visualize the retinal capillary layer in healthy eyes. We also compared reflectance confocal AO-SLO with OCTA in imaging retinal layered capillaries.

## Methods

This study was approved by the Institutional Ethics Committees of the Kyushu University Hospital (Protocol No. 25233, UMIN000016858), and was performed in accordance with the ethical standards laid down by the Declaration of Helsinki. Written informed consent was obtained from all patients after a detailed explanation of the study.

### Participants

The study included 16 healthy subjects (10 eyes of 10 females and 6 eyes of 6 males) with clear ocular media and no history of prior ocular or systemic disease.

## Adaptive Optics Scanning Laser Ophthalmoscopy (AO-SLO)

Patients underwent full ophthalmologic examination including slit-lamp examination, dilated fundus examination, and color fundus photography to confirm no apparent retinal disorder after pupil dilatation with an eye drop of 0.5 % tropicamide and 0.5 % phenylephrine (Mydrin-P; Santen, Osaka, Japan). Based on a previous report,<sup>25</sup> axial length was measured in each patient using IOL master (Carl Zeiss Meditec, Jena, Germany) to calculate the AO-SLO image scale. In addition, all patients underwent imaging using a prototype AO-SLO system (depth of focus:  $\sim 60$   $\mu\text{m}$ ; Canon, Inc., Tokyo, Japan) as described previously.<sup>23</sup> The AO-SLO device consists of an adaptive optics system that can measure and compensate optical aberrations produced by ocular media, a high-resolution confocal SLO imaging system, and a wide-field imaging subsystem. The wavelength of AO-SLO is 845 nm, and the wavelength of the beacon light for measurement of wavefront aberrations is 760 nm. The imaging light and the beacon light power are set at 400 and 100  $\mu\text{W}$ , respectively, in accordance with the safety limits set by the American National Standards Institute. The optical resolution is 5  $\mu\text{m}$ .

### Image Acquisition with AO-SLO

We imaged retinal vascular networks in the macular area ( $2.8 \times 2.8$  mm) of all subjects using a prototype AO-SLO system. The movies were recorded for 3 seconds per scan area with a field size of  $2.8^\circ \times 2.8^\circ$  at 25 regions. The frame rate was 32 frames per second. The AO-SLO device can focus on the photoreceptor layer as well as capillaries in the nerve fiber layer while compensating for aberrations of the target eye, and automatically create an en face image in each movie. Each area was imaged in succession. If the imaging conditions were poor (poor fixation or blinking), these areas were imaged again. The layer adjustment range in the AO-SLO device is  $\pm 2$  diopters (D) from the photoreceptor layer. Therefore, the AO-SLO device allows the creation of an en face image of the photoreceptor and nerve fiber layers.

### Motion Contrast Enhancement in AO-SLO Imaging

The capillary images were constructed by AO-SLO Retinal Image Analyzer software (ARIA; Canon, Inc.) dedicated to the prototype AO-SLO. The ARIA

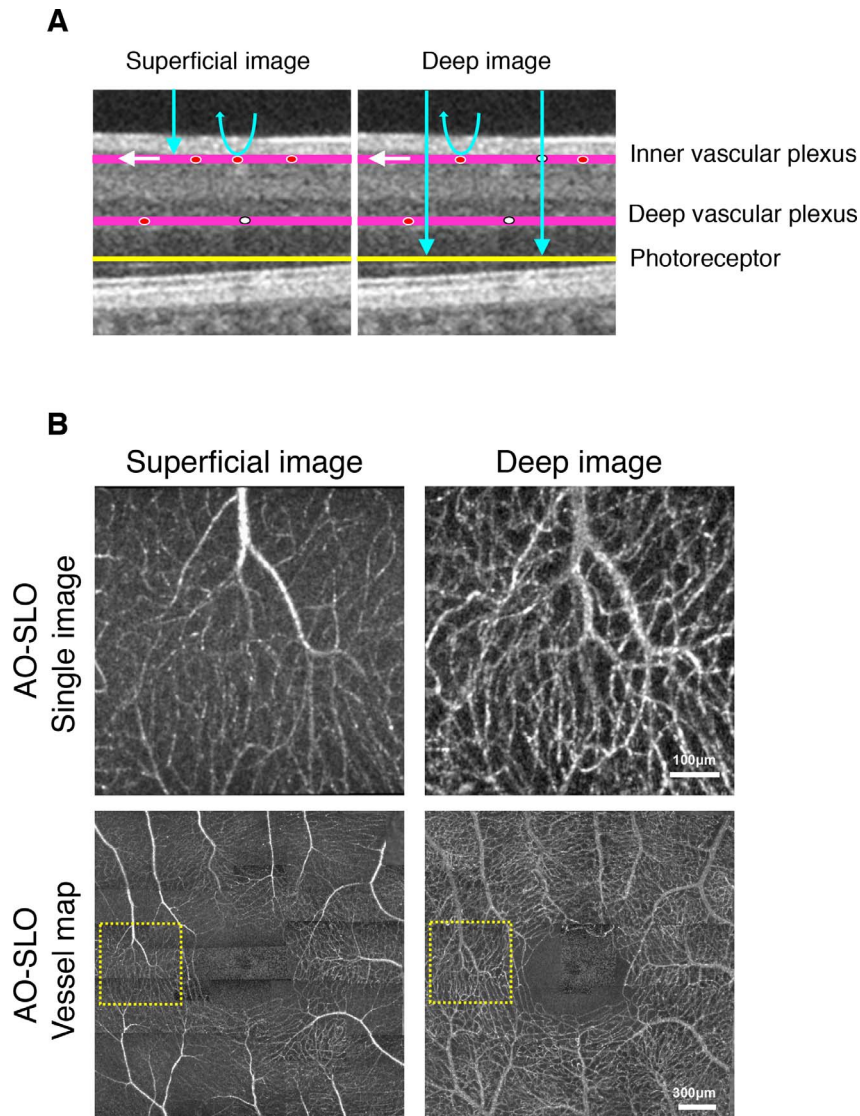


**Figure 1.** Imaging of the hierarchical structure of retinal vessels with AO-SLO. (A) The vessels are shown in *pink*. The scanning lights are shown in *blue*. The photoreceptor layer is shown in *yellow*. *Red* and *white circles* indicate red blood cells and leukocytes, respectively. (B) When focusing on the retinal nerve fiber layer, superficial retinal vasculatures could be imaged as a superficial image with AO-SLO. When focusing on the photoreceptor layer, we could also image all retinal vasculatures as a deep image with AO-SLO. Twenty-five single images were merged to make a 2.8-mm square vessel map in each of the two different layers using ARIA. *Yellow dotted squares* indicate an AO-SLO single image.

software adopts the same methods that was published in a paper by Tam et al.<sup>20</sup>

### Imaging of the Hierarchical Structure of Retinal Vessel with AO-SLO

When the AO-SLO device was focused on the photoreceptor layer and on the capillaries at the nerve fiber layer, flickering could be observed in the vessel. The flickering at the nerve fiber layer could have originated from red blood cells in the superficial vessels (superficial image), whereas the flickering

when focusing on the photoreceptor could have originated from the whole vessels in the retina (deep image; Figs. 1A, 1B). As reported previously,<sup>26</sup> when red blood cells are present in the light path, the light cannot reach the photoreceptor because of the hemoglobin. On the other hand, when leukocytes are present in the light path, the light can reach the photoreceptor because of the transparency. As both red blood cells and leukocytes flow through blood vessels, flickering occurs in the AO-SLO image (Figs. 1A, 2B). Twenty-five pictures were merged to make a



2.8-mm<sup>2</sup> vessel map in each of the two different layers with ARIA (Fig. 1B).

### Vessel Depth of AO-SLO Imaging

To distinguish the two different layered vessel structures, the superficial and deep capillary images, which were constructed by ARIA, were converted to green and red, respectively (Figs. 2A, 2B). These two images were merged into a single image using Image J 1.48 software (<http://imagej.nih.gov/ij/>; provided in the public domain by the National Institutes of Health, Bethesda, MD, USA) (Fig. 2B).

### Optical Coherence Tomography Angiography (OCTA)

We imaged retinal vascular networks of all subjects using OCTA (Optovue RTVue XR Avanti; Optovue, Inc., Fremont, CA) and obtained retinal vascular mapping images of the macular area (3.0 × 3.0 mm) on the same day of AO-SLO imaging. The instrument was used to obtain split-spectrum amplitude decorrelation angiography (SSADA) images.<sup>6</sup> The instrument has an A-scan rate of 70,000 scans per second, using a light source centered on 840 nm and a band-width of 45 nm. The tissue resolution is 5- $\mu$ m axially, and there is a 22- $\mu$ m beam width. Each B-scan contained 216 A-scans. Five consecutive B-scans (M-B frames) were captured at a fixed position before proceeding to the next sampling location. A total of 216 locations (B-scans) along the slow transverse direction were sampled to form a three-dimensional data cube. With a B-scan frame rate of 270 frames per second, the 1080 B-scans in each scan sequence were acquired in approximately 4 seconds. Four volumetric raster scans, including two horizontal priority fast transverse (x-fast) scans and two vertical priority fast transverse (y-fast) scans, were obtained consecutively in one session. The best x-fast and y-fast scans were registered using the contained software (ReVue; Optovue, Inc.), which has the ability to correct some motion artifacts, including residual axial motion and transverse saccadic motion. After processing of the volume scans, the decorrelation in the images, which is essentially one minus the correlation, was calculated. Stationary tissue shows a high correlation in imaging characteristics from one frame to the next. Blood flowing through vessels causes a changing reflectance over time and localized areas of low correlation between frames (or conversely a high decorrelation). This method does not use phase information from the OCTA signal. The correlated frames were evaluated and statistical outliers were

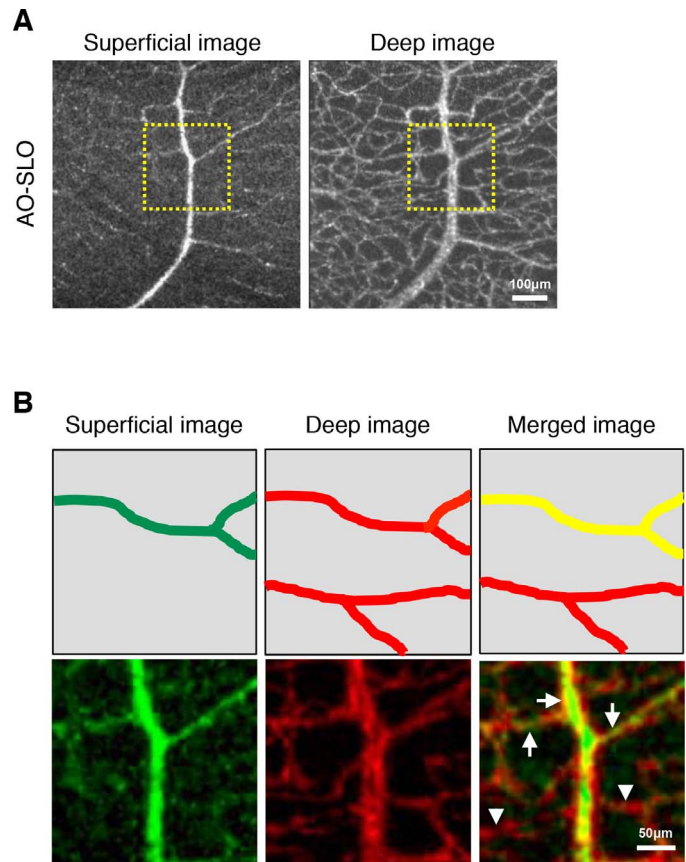


**Figure 2.** Distinction of different layered retinal vessels using AO-SLO images. (A) The superficial and deep capillary AO-SLO images were constructed using ARIA. (B) To distinguish the two different layered vessels, the superficial and deep images were converted to *green* and *red*, respectively. Yellow vessels indicated by *arrows* are in the superficial layer, whereas red vessels indicated by *arrowheads* are in the deep layer. *Yellow dotted squares* indicate the AO-SLO image in (B).

removed from the averaging process to reduce the possibility of tissue motion being present. The spectrum of the light source was split into four component parts to decrease the noise present in the image; each was used to perform the decorrelation step, and the results of all four were averaged. This split-spectrum strategy trades axial resolution for decreased noise. After this step, a block of information exists that contains levels of decorrelation that range from 0 to 1. In any given region of tissue, the maximal projection image can be viewed to obtain an image of the contained blood flow. As the retina is a laminar structure with a corresponding stratification of the blood supply, segmentation of the retina in specific layers allows simple en-face visualization of the corresponding vascular supply for that layer. While we could obtain four types of vascular mapping images

of each layer of retina using OCTA (as superficial, deep, outer retina, and choriocapillaris layers), we used the superficial (upper: inner limiting membrane with offset of 3  $\mu\text{m}$ , lower: inner plexiform layer [IPL] with offset of 15  $\mu\text{m}$ ) and deep layer images (upper: IPL with offset of 15  $\mu\text{m}$ , lower: IPL with offset of 70  $\mu\text{m}$ ) for the current investigation.

### Foveal Avascular Zone (FAZ) Quantification

The foveal avascular zone (FAZ) boundary was defined as the inner edge of the bordering vessels. With one side of the OCTA image being 3 mm, FAZ in OCTA was manually measured using ImageJ 1.48 software. Two independent researchers (YK and SN) assessed if the AO-SLO images were merged correctly for the measurement of the FAZ area. The FAZ in the merge image of AO-SLO was calculated using the distance calculated from one side (3 mm) of OCTA image. The statistical analyses (paired *t*-test) were performed using the software, JMP v10.0 (SAS Institute, Cary, NC).

### Estimation of AO-SLO Images at the 0.5- and 1.0-mm Area From the Fovea

We investigated whether the quality of 64 AO-SLO images ( $820 \times 820 \mu\text{m}$ ) at the distance of 0.5 and 1.0 mm from the fovea in the superior, inferior, nasal, and lateral location was sufficient for image analysis. The quality of retinal vascular mapping images of AO-SLO was evaluated independently by two observers (YK and IW). In cases where the evaluation of the two observers was different, a third observer (MY) evaluated the image quality. The kappa coefficient was 0.64 and 0.78 ( $P < 0.001$  and  $P < 0.0001$ ) for estimation of the image quality at the distance of 0.5 and 1.0 mm from the fovea as defined above, respectively.

### Comparison of AO-SLO and OCTA

The superficial and deep vascular images of OCTA in the same area where good quality AO-SLO images were chosen were cropped with Keynote (Apple Corp., Cupertino, CA). We evaluated the two images as follows: two researchers (YK and IW) independently compared AO-SLO and OCTA images, and counted the number of different vascular structures in the images; and each image was scored as follows: (1) in cases whereby the vessel was detectable only on either an AO-SLO image or an OCTA image but not both, the image was scored “+1” if the number of superior quality points was greater in an AO-SLO image than in

an OCTA image, and scored “-1” if it was greater in an OCTA image than in an AO-SLO image; and (2) regardless of a difference in the number of superior quality points, the image was scored “0” if there was at least one superior quality point in both AO-SLO and OCTA images. Because eight pairs of corresponding images obtained by AO-SLO and OCTA were evaluated in each case, the highest and lowest score were +8 and -8, respectively. Data were examined by the Wilcoxon one-sample signed rank test and the median, standard deviation (SD), and *P* value were calculated. The kappa coefficient was 0.93 and 0.75 ( $P < 0.0001$  and  $P < 0.0001$ ) at the distance of 0.5 and 1.0 mm from the fovea for estimation of the two images as defined above, respectively. This result indicated good interobserver agreement. The superiority was analyzed using the Wilcoxon signed-rank test.

### Estimation of Imaged Vascular Layer in AO-SLO

In AO-SLO merged images (as shown in Fig. 1B) at 1.0 mm from the fovea, three superficial and three deep vessels were randomly chosen. Two researchers (YK and IW) estimated the AO-SLO-imaged vascular layer with the corresponding OCTA images. The kappa coefficient was 1.0. The concordance rate was calculated for estimation of both superficial and deep vessels. Furthermore, the width of the vessels that AO-SLO but not OCTA could image was measured with ARIA. The lumen diameter at the next branch that both AO-SLO and OCTA could image was also measured with ARIA in AO-SLO vessel maps extracted from the photoreceptor videos.

### Statistical Analysis

Statistical analyses were performed using the software, JMP v10.0 (SAS Institute). Continuous variables were analyzed using the Wilcoxon signed-rank test or two-sample *t*-test as appropriate. Categorical variables were assessed using Fisher's exact test. *P* values less than 0.05 were considered statistically significant.

## Results

### Subject Characteristics

The average subject age was 26.7 years with a SD of 2.2 years. Ten subjects were females (62.5%). The average axial length was  $25.4 \pm 1.7$  mm. Participant characteristics in this study are summarized in Table 1.

**Table 1.** Basic Characteristics of the Subjects

Characteristics	
No. of eyes (participants)	16 (16)
Mean age $\pm$ SD, y (range)	26.6 $\pm$ 2.3 (23–31)
Sex, male:female	6:10
Axial length, mm	25.4 $\pm$ 1.6

### Imaging of Layered Retinal Vascular Networks Using AO-SLO

When focusing on the retinal nerve fiber layer, superficial retinal vasculatures could be imaged (superficial image; Figs. 1A, 1B). When focusing on the photoreceptor layer, we could also image all retinal vasculatures (deep image; Figs. 1A, 1B). Thicker vessels of the superficial layer of the retina were imaged clearly in the superficial image. Part of capillary network in the inner vascular plexus could not be imaged well in the superficial image. Capillaries as well as thicker vessels could also be imaged in the deep image. Retinal vessels could be imaged thinner and brighter in the superficial image than in the deep image (Fig. 1B). These data indicate that AO-SLO could image retinal vessels in the superficial layer and in all layers by using a different focusing method.

### Distinguishing Different Layered Retinal Vessels Using AO-SLO Images

To distinguish the two different layered vasculatures, the superficial and the deep images were

converted to green and red, respectively, and these two images were merged (Fig. 2). In the merged image, yellow indicates superficial vessels, whereas red indicates deep vessels (Fig. 2B). This data suggest retinal vessels in different layers could be distinguished using AO-SLO images (Table 2).

### Quantitative Comparison between AO-SLO and OCTA

Among 16 cases (each comprising 64 images taken at the distance of 0.5 and 1.0 mm from the fovea), we assessed that seven cases (43.8%: five eyes of five females and two eyes of two males) included images of sufficient quality for analysis while the AO-SLO images from the nine cases that were not analyzed contained insufficient image quality for the analysis (Table 2). Seventeen superficial images (26.6%) taken at 0.5-mm distance were good enough for analysis (Fig. 3A), and 14 taken at the 1.0-mm distance (21.9%) were judged to be good enough for analysis (Figs. 3B, 3C). The AO-SLO merged image was able to show retinal vessel structures similar to OCTA (Figs. 3D–G).

### Quantitative Comparison of Vessel Structure Imaging between AO-SLO and OCTA

Retinal vasculatures at the distance of 0.5 mm from the fovea form the foveal vascular zone (Fig. 4), whereas retinal vasculatures at the distance of 1.0 mm from the fovea consist of a two-layered structure (Fig. 5). Next, we compared AO-SLO images with OCTA at distances of 0.5 and 1.0 mm from the fovea. As reported previously,<sup>24</sup> retinal vessels in OCTA images

**Table 2.** Summary of Research Results: Comparison of AO-SLO and OCTA

	AO-SLO	OCT Angiography	P Value
Dye injection	Unnecessary	Unnecessary	NA
Lateral optical resolution, $\mu$ m	5	20	NA
Lateral image resolution, $\mu$ m	2	13.9	NA
Distinction of layer structure	Possible*	Possible	NA
Sufficient quality image, %	43.8	100	NA
Vessel structure imaging (0.5 mm from the fovea)	The ability of AO-SLO is superior compared with OCTA (+2.5 $\pm$ 2.7 points†)		0.03
Vessel structure imaging (1.0 mm from the fovea)	The ability of AO-SLO is superior compared with OCTA (+2.5 $\pm$ 1.9 points†)		0.02
FAZ area (mm <sup>2</sup> )	0.36 $\pm$ 0.12	0.34 $\pm$ 0.11	0.08

NA, not analyzed.

\* 40.5% of vessels that AO-SLO recognized as the deep layer are imaged in the superficial vessel layer in OCTA.

† Our quantitative analysis shows the ability of AO-SLO to visualize vessels is significantly superior compared to OCTA at both 0.5 and 1.0 mm from the fovea. The quantitative method is shown in Methods.



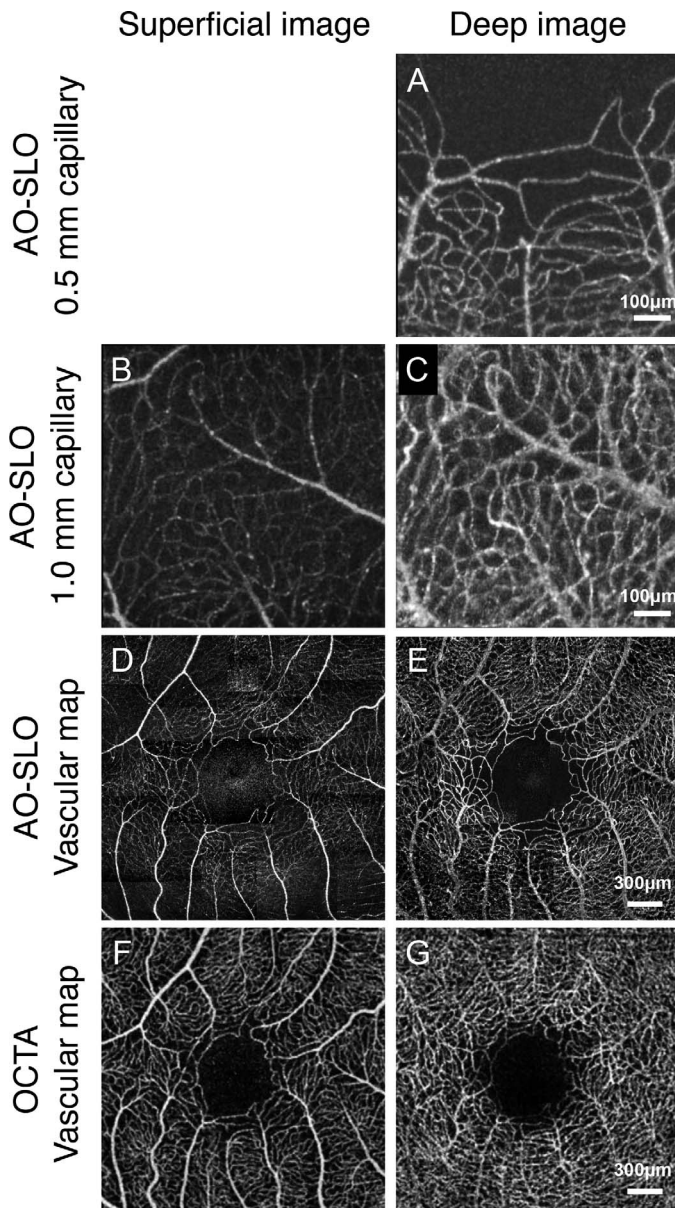


**Figure 3.** Imaging of parafoveal monolayered and multilayered retinal vessels using AO-SLO. (A, C) When focusing on the photoreceptor layer, we could image all retinal vasculatures as a deep image at 0.5 (A) and 1.0 mm (C) from the fovea with AO-SLO. (B) When focusing on the retinal nerve fiber layer, superficial retinal vasculatures could be imaged as a superficial image at 1.0 mm from the fovea with AO-SLO. (D, E) Twenty-five AO-SLO images were merged to make a 2.8-mm square vessel map in each of the two different layers with ARIA. The superficial and deep images are shown as D and E, respectively. (F, G) OCT angiography from the same eye is shown (F; superficial retinal image, G; deep retinal image).

tend to be imaged thicker than those in our prototype AO-SLO (Figs. 4 and 5). Although the differences in the width of each capillary were clearly distinguished in AO-SLO, those differences were unclear in OCTA

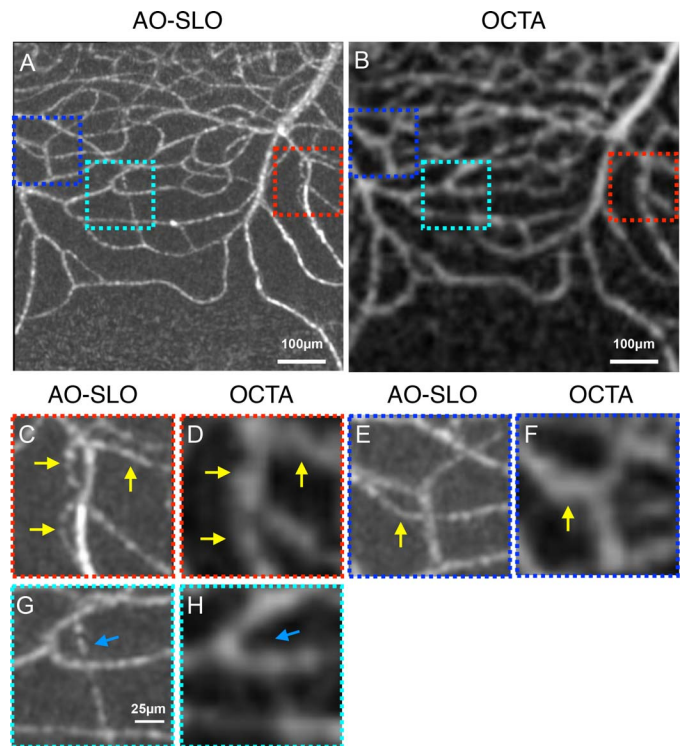


**Figure 4.** Comparison of foveal microvasculatures imaging between AO-SLO and OCTA. (A, C, E, G) Representative retinal vascular images in the superior area 0.5 mm from the fovea was acquired by focusing on the photoreceptor layer with AO-SLO. (B, D, F, H) The same area was cropped from the OCTA image. *Yellow arrows* indicate close-running capillaries, which could be distinguished from each other in the AO-SLO image but not in the OCTA image. The *blue arrow* indicates a capillary that could not be imaged by OCTA but was imaged by AO-SLO.

at 0.5 as well as 1.0 mm from the fovea (Figs. 4 and 5). Close-running capillaries could also be distinguished from each other in AO-SLO images, whereas these capillaries were imaged as single-thick capillaries in OCTA images (Figs. 4C–F, and 5C, 5D). Some capillary structures, which were simply seen as branching structures in OCTA images, could be imaged as doughnut-shape structures in AO-SLO images (Figs. 5E, 5F). Furthermore, some capillaries could not be imaged by OCTA while they could be imaged by AO-SLO (Figs. 4G, 4H). However, a few capillaries could be imaged by OCTA but not by AO-SLO (Fig. 6). Our quantitative analysis showed that the ability of AO-SLO to visualize vessels was significantly superior compared with OCTA at both 0.5 and 1.0 mm from the fovea (median  $\pm$  SD;  $+2.5 \pm 2.7$  points and  $+2.5 \pm 1.9$  points,  $P = 0.03$  and  $0.02$ , respectively; Table 2).

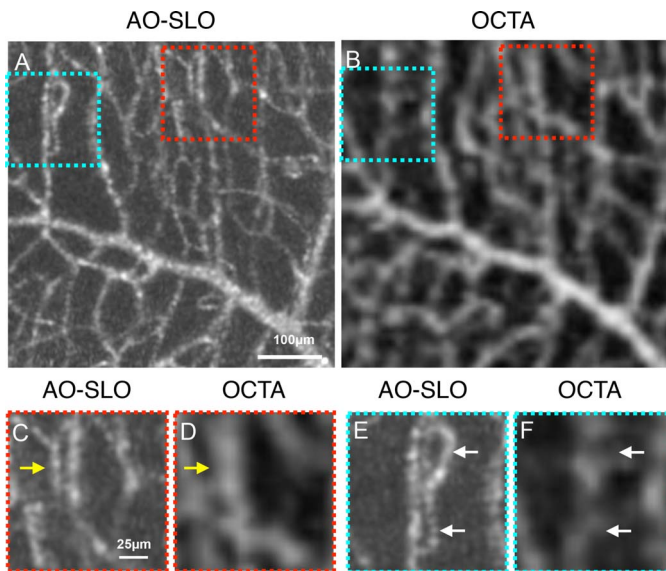


**Figure 5.** Comparison of layered microvasculatures imaging between AO-SLO and OCTA. (A, C, E) Representative retinal vascular images in the nasal area 1.0 mm from the fovea was acquired by focusing on the photoreceptor layer with AO-SLO. (B, D, F) The same area was cropped from the OCTA image. *Yellow arrows* indicate close-running capillaries, which could be distinguished from each other in the AO-SLO image but not in the OCTA image. *White arrows* indicate doughnut-shape structures of the retinal capillary network that could not be imaged by OCTA but were imaged by AO-SLO.

### Lumen Diameter of AO-SLO Imaged Vessels

The lateral optical resolution of our prototype AO-SLO is higher than the optical resolution of commercial OCTA.<sup>23</sup> To examine if the higher resolution could explain the superior vessel plot-out ability of AO-SLO compared with OCTA, the lumen diameter was measured with our AO-SLO image analyzer. The lumen diameter of the vessels that AO-SLO, but not OCTA, could image ( $10.2 \pm 2.8 \mu\text{m}$ ,  $n = 15$ ) was similar to one of the vessels at the next branch, which both AO-SLO and OCTA could image ( $10.1 \pm 2.4 \mu\text{m}$ ,  $n = 15$ ) on the vessel maps extracted from the photoreceptor ( $P = 0.95$ ).

### Quantitation of Foveal Avascular Zone with AO-SLO and OCTA

Next, we compared the area of the FAZ among AO-SLO and OCT images. Our quantitative analysis showed that there was no significant difference between the FAZ area in AO-SLO ( $0.36 \pm 0.12 \text{ mm}^2$ ) and in OCTA ( $0.34 \pm 0.11 \text{ mm}^2$ ;  $P = 0.08$ , Fig. 7, Table 2).

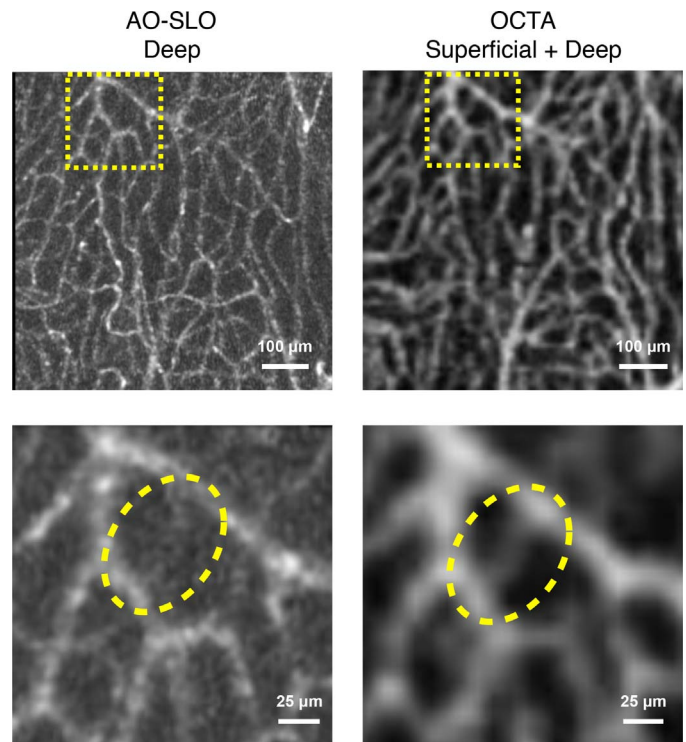


**Figure 6.** Capillaries imaged by OCTA but not AO-SLO. (Left) Representative retinal vascular images in the temporal area 1.0 mm from the fovea was acquired by focusing on the photoreceptor layer with AO-SLO. (Right) The same area was cropped from the OCTA image. *Yellow dotted circles* indicate a capillary, which could be imaged by OCTA but not by AO-SLO.

### Comparison of Vessel Layer between AO-SLO and OCTA

Lastly, we investigated differences in the imaged vascular layer between AO-SLO and OCTA. All vessels that were recognized as the superficial layer in AO-SLO, were imaged in the superficial vessel layer in OCTA. However, 40.5% of vessels, which AO-SLO recognized as the deep layer was imaged in the superficial vessel layer in OCTA (Table 2). These data indicate that the superficial vascular layers could be consistent between AO-SLO and OCTA, whereas the deep vascular layer in AO-SLO included the OCTA superficial vascular image.

## Discussion

Recently, there have been various reports demonstrating the usefulness of OCTA as a tool for clinical evaluations in retinal vascular disorders.<sup>6,8,27</sup> OCTA provides both structural and functional (i.e., blood flow) information of retinal vasculatures. A distin-



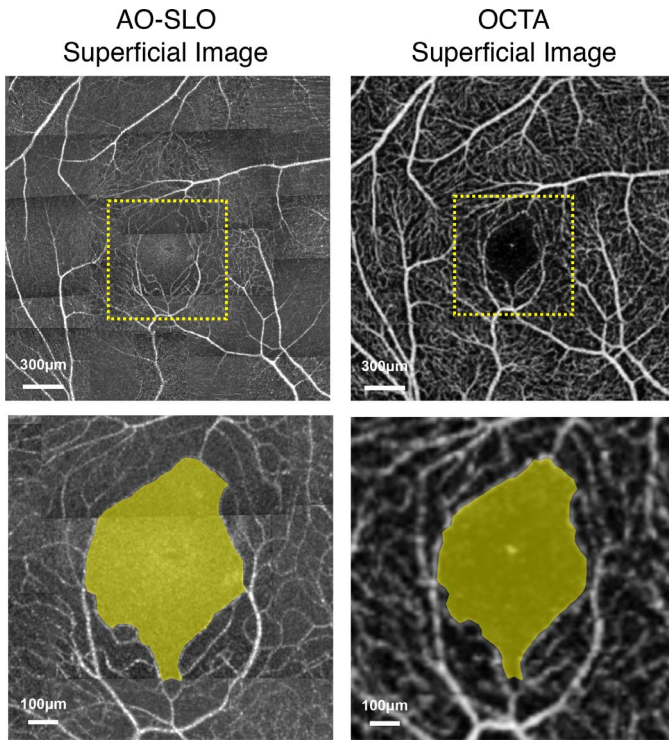


**Figure 7.** Comparison of foveal avascular zone imaging between AO-SLO and OCTA. AO-SLO (left column) and OCTA (right column) images centered at the fovea in a healthy subject. Top; merged AO-SLO and cropped OCTA. Yellow dotted squares indicate higher magnification area in the bottom. Yellow area indicates measured areas for the analysis.

guishing feature of OCTA that differs from existing imaging equipment is its ability to image retinal vascular layers.<sup>8</sup> In this study, we investigated the potential of AO-SLO for imaging the retinal vascular layer in healthy eyes. As the depth of focus of our prototype AO-SLO is approximately 60  $\mu\text{m}$ , AO-SLO has excellent representation of a specific layer structure, such as the photoreceptor layer.<sup>12–16</sup> To distinguish the retinal vascular layers, we performed a method that subtracts superficial vascular images from images that include both vascular layers. Using this method, the distinction of the superficial retinal vessels and deep retinal vessels was possible in high resolution. However, it was more difficult to image the hierarchical structure compared with OCTA. Only 43.8% AO-SLO images were of sufficient quality for use in this current study (Table 2). This could be due to eye motion or an unstable tear film. Furthermore, disorder of the retinal layer structure in an image area could also influence the method. Although the healthy eye could be investigated in this study, retinal diseases such as edema and high myopia might pose

difficulty in imaging the layered retinal vascular networks.

A clinical gold standard in imaging the retinal vessels has still been FA. However, it is known that angiography using an injected dye sometimes can lead to adverse events including anaphylaxis.<sup>3</sup> Therefore, a novel method to image retinal capillaries is desirable. The best feature of OCTA could be its ability to visualize the flow without using an injected dye. A recent study that compared AO-SLO with OCTA also used fluorescein for the AO-SLO.<sup>24</sup> Two methods to image retinal vessels using AO-SLO have been reported. One method was AO-SLO FA using injected dye and the other method was AO-SLO using motion contrast, which were introduced by Pinhas<sup>28</sup> and Tam<sup>20</sup>, respectively. In this study, we investigated the ability to image retinal vessels by observing the retinal vessels using motion contrast in AO-SLO instead of injected dyes. We confirmed that retinal vessels that could not be visualized with the OCTA could be observed with our prototype AO-SLO. Specifically, close-running capillaries as well as doughnut-shaped vessel structures could not be imaged well in OCTA. Our observation is consistent with a recent study using AO-SLO FA.<sup>24</sup> Therefore, similar to AO-SLO FA, AO-SLO with motion contrast is also useful in imaging retinal capillaries without any dye. Furthermore, although the utility of AO-SLO FA in imaging the hierarchical structure of retinal capillaries has not yet been examined, the method introduced in this study might be also available for AO-SLO FA.

As the lateral optical resolution of AO-SLO (5  $\mu\text{m}$ ) is around four times higher than OCTA (20  $\mu\text{m}$ ; Table 2), the superiority of the vessel plot-out ability of AO-SLO could be due to the resolution. However, the diameter of vessels that OCTA was unable to image was not smaller than the diameter of the vessels that were observed in this study. Another possible reason is the difference in imaging frame rate. The frame rate of AO-SLO is known to be 32 frames per second (96 frames in three seconds imaging), whereas the OCTA frame rate could be 1.3 to 1.4 frames per second (4 frames in 3-second imaging) that is lower than AO-SLO.

Diameter differences of each retinal vessel could be observed with AO-SLO while OCTA tends to equalize the vessel thickness. The lateral image resolution is 2  $\mu\text{m}$  in AO-SLO, whereas it is 13.9  $\mu\text{m}$  in OCTA (Table 2). Therefore, it was thought that there is a tendency for OCTA to equalize without depicting differences in vessel diameter. However, it

may be difficult to simply compare the diameter of the retinal vessel between the AO-SLO images and OCTA images. As the AO-SLO device creates en face images, retinal vessels could be imaged thicker in the deep image than in the superficial image. Thus, the retinal vessel diameter is dependent on the depth of the imaged vessels. Therefore, measurement of vessel diameter using AO-SLO might be of limited use. It is expected that a method to measure the diameter that is corrected for the depth would be developed. However, because the imaged vessels in AO-SLO are derived from the flow using motion contrast, the imaged lumen diameter cannot be equal to the actual anatomic diameter.

Based on previous reports, FAZ was clearly recognized and quantifiable in this study. A recent report showed that the area of FAZ on the OCTA is larger than that on AO-SLO when quantified.<sup>24</sup> However, our quantification did not show this difference (Table 2). This might be due to the AO-SLO FA in the previous reports.<sup>24</sup> Due to leakage in AO-SLO FA, it is likely to be smaller than the real image. In addition, diseased eyes were included in the previous reports.<sup>24</sup> Although the presence or absence of axis length correction, difference in analysis software, and image merging might affect the FAZ measurement, the difference in FAZ area may also occur in AO-SLO due to difference in blood vessel imaging method (FA and motion contrast).

This study has the limitations inherent in any study of limited sample size. A dedicated adaptive optics instrument is used to acquire a large number of images, and this is followed by image averaging, which in turn is followed by montaging separate images to obtain a field of view large enough to have clinical utility. Furthermore, this study evaluated the ability of AO-SLO to visualize the retinal vascular layer only in healthy eyes. Despite this, we could only analyze half of all images (Table 2). Therefore, it would likely be even more difficult in diseased eyes.

## Acknowledgments

The authors thank Kazushi Nomura and Takeshi Kitamura (Canon, Inc.) for their technical support.

Supported by grants from JSPS KAKENHI, Grant-in-Aid for Young Scientists (A) No. 25713057 (SN) and Grant-in-Aid for Scientific Research (C) No. 17K11456 (SN).

Disclosure: **Y. Kaizu**, None; **S. Nakao**, None; **I. Wada**, None; **M. Yamaguchi**, None; **K. Fujiwara**, None; **S. Yoshida**, None; **T. Hisatomi**, None; **Y. Ikeda**, None; **T. Hayami**, None; **T. Ishibashi**, None; **K.-H. Sonoda**, None

## References

1. Hughes S, Yang H, Chan-Ling T. Vascularization of the human fetal retina: roles of vasculogenesis and angiogenesis. *Invest Ophthalmol Vis Sci*. 2000;41:1217–1228.
2. Novotny HR, Alvis DL. A method of photographing fluorescence in circulating blood in the human retina. *Circulation*. 1961;24:82–86.
3. Yannuzzi LA, Rohrer KT, Tindel LJ, et al. Fluorescein angiography complication survey. *Ophthalmology*. 1986;93:611–617.
4. Mendis KR, Balaratnasingam C, Yu P, et al. Correlation of histologic and clinical images to determine the diagnostic value of fluorescein angiography for studying retinal capillary detail. *Invest Ophthalmol Vis Sci*. 2010;51:5864–5869.
5. Kwiterovich KA, Maguire MG, Murphy RP, et al. Frequency of adverse systemic reactions after fluorescein angiography. Results of a prospective study. *Ophthalmology*. 1991;98:1139–1142.
6. Ishibazawa A, Nagaoka T, Takahashi A, et al. Optical coherence tomography angiography in diabetic retinopathy: a prospective pilot study. *Am J Ophthalmol*. 2015;160:35–44, e31.
7. Nakao S, Kaizu Y, Oshima Y, Sakamoto T, Ishibashi T, Sonoda KH. Optical coherence tomography angiography for detecting choroidal neovascularization secondary to punctate inner choroidopathy. *Ophthalmic Surg Lasers Imaging Retina*. 2016;47:1157–1161.
8. Spaide RF, Klancnik JM Jr, Cooney MJ. Retinal vascular layers imaged by fluorescein angiography and optical coherence tomography angiography. *JAMA Ophthalmol*. 2015;133:45–50.
9. Rha J, Jonnal RS, Thorn KE, Qu J, Zhang Y, Miller DT. Adaptive optics flood-illumination camera for high speed retinal imaging. *Opt Express*. 2006;14:4552–4569.
10. Weinhaus RS, Burke JM, Delori FC, Snodderly DM. Comparison of fluorescein angiography with microvascular anatomy of macaque retinas. *Exp Eye Res*. 1995;61:1–16.
11. Roorda A, Romero-Borja F, Dornelly W, Iii Queener H, Hebert T, Campbell M. Adaptive

- optics scanning laser ophthalmoscopy. *Opt Express*. 2002;10:405–412.
12. Yamaguchi M, Nakao S, Kaizu Y, et al. High-resolution imaging by adaptive optics scanning laser ophthalmoscopy reveals two morphologically distinct types of retinal hard exudates. *Sci Rep*. 2016;6:33574.
  13. Kaizu Y, Nakao S, Yamaguchi M, Murakami Y, Salehi-Had H, Ishibashi T. Detection of airbag impact-induced cone photoreceptor damage by adaptive optics scanning laser ophthalmoscopy: a case report. *BMC Ophthalmol*. 2016;16:99.
  14. Ooto S, Hangai M, Takayama K, et al. High-resolution imaging of the photoreceptor layer in epiretinal membrane using adaptive optics scanning laser ophthalmoscopy. *Ophthalmology*. 2011; 118:873–881.
  15. Talcott KE, Ratnam K, Sundquist SM, et al. Longitudinal study of cone photoreceptors during retinal degeneration and in response to ciliary neurotrophic factor treatment. *Invest Ophthalmol Vis Sci*. 2011;52:2219–2226.
  16. Nakao S, Kaizu Y, Yoshida S, Iida T, Ishibashi T. Spontaneous remission of acute zonal occult outer retinopathy: follow-up using adaptive optics scanning laser ophthalmoscopy. *Graefes Arch Clin Exp Ophthalmol*. 2015;253:839–843.
  17. Roorda A, Williams DR. The arrangement of the three cone classes in the living human eye. *Nature*. 1999;397:520–522.
  18. Carroll J, Baraas RC, Wagner-Schuman M, et al. Cone photoreceptor mosaic disruption associated with Cys203Arg mutation in the M-cone opsin. *Proc Natl Acad Sci U S A*. 2009;106:20948–20953.
  19. Tam J, Dhamdhere KP, Tiruveedhula P, et al. Disruption of the retinal parafoveal capillary network in type 2 diabetes before the onset of diabetic retinopathy. *Invest Ophthalmol Vis Sci*. 2011;52:9257–9266.
  20. Tam J, Martin JA, Roorda A. Noninvasive visualization and analysis of parafoveal capillaries in humans. *Invest Ophthalmol Vis Sci*. 2010;51: 1691–1698.
  21. Burns SA, Elsner AE, Chui TY, et al. In vivo adaptive optics microvascular imaging in diabetic patients without clinically severe diabetic retinopathy. *Biomed Opt Express*. 2014;5:961–974.
  22. Chui TY, Pinhas A, Gan A, et al. Longitudinal imaging of microvascular remodelling in proliferative diabetic retinopathy using adaptive optics scanning light ophthalmoscopy. *Ophthalmic Physiol Opt*. 2016;36:290–302.
  23. Hirose F, Nozato K, Saito K, Numajiri Y. A Compact adaptive optics scanning laser ophthalmoscope with high-efficiency wavefront correction using dual liquid crystal on silicon - spatial light modulator. *Proc Spie*. 2011; 7885.
  24. Mo S, Krawitz B, Efsthadiadis E, et al. Imaging foveal microvasculature: optical coherence tomography angiography versus adaptive optics scanning light ophthalmoscope fluorescein angiography. *Invest Ophthalmol Vis Sci*. 2016;57: OCT130–OCT140.
  25. Bennett AG, Rudnicka AR, Edgar DF. Improvements on Littmann's method of determining the size of retinal features by fundus photography. *Graefes Arch Clin Exp Ophthalmol*. 1994;232:361–367.
  26. Uji A, Hangai M, Ooto S, et al. The source of moving particles in parafoveal capillaries detected by adaptive optics scanning laser ophthalmoscopy. *Invest Ophthalmol Vis Sci*. 2012;53:171–178.
  27. Takase N, Nozaki M, Kato A, Ozeki H, Yoshida M, Ogura Y. Enlargement of foveal avascular zone in diabetic eyes evaluated by en face optical coherence tomography angiography. *Retina* 2015; 35:2377–2383.
  28. Pinhas A, Dubow M, Shah N, et al. In vivo imaging of human retinal microvasculature using adaptive optics scanning light ophthalmoscope fluorescein angiography. *Biomed Opt Express*. 2013;4:1305–1317.